Figure S1. Western blot validation of APP, α-synuclein A53T, and Q74 overexpression in SH-SY5Y cells. (A) Representative Western blot analysis of APP expression in Ctrl and APP-overexpressing SH-SY5Y cells. (B) Quantitative analysis of APP protein expression normalized to β-actin. (C) Representative western blot analysis of α-synuclein expression in Ctrl and A53T-overexpressing SH-SY5Y cells. (D) Quantitative analysis of α-synuclein protein expression normalized to β-actin. (E) Representative Western blot analysis of GFP expression in Ctrl and Q74-overexpressing SH-SY5Y cells. GFP was used to detect GFP-tagged Q74 expression. (F) Quantitative analysis of GFP protein expression normalized to β-actin. Data are presented as the mean ± SEM. ***P<0.001 vs. Ctrl. APP, amyloid precursor protein; GFP, green fluorescent protein.

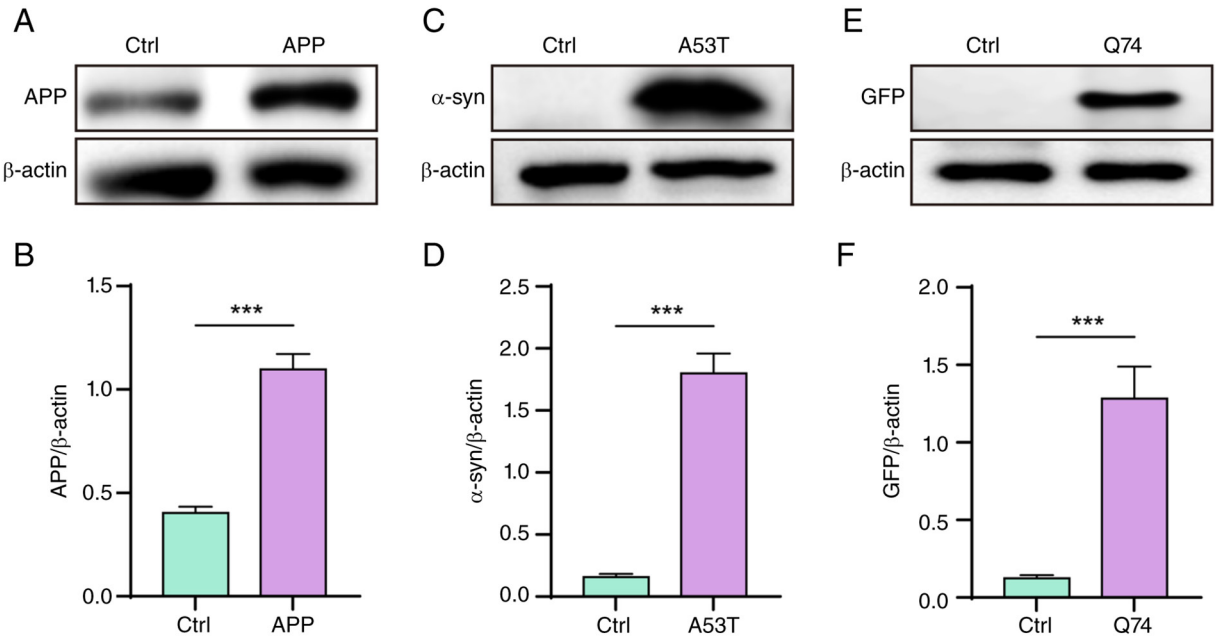

Figure S2. Fer-1 rescues cell viability loss and cell death in APP-overexpressing SH-SY5Y cells. (A) Quantitative analysis of cell viability in APP-overexpressing SH-SY5Y cells treated with or without Fer-1 (0.2 μM). (B) Representative Hoechst/PI staining images of APP-overexpressing SH-SY5Y cells treated with or without Fer-1. Magnification, x10; scale bars, 50 μm. (C) Quantitative analysis of cell death rate. Data are presented as the mean ± SEM. ***P<0.001. Fer-1, ferrostatin-1; APP, amyloid precursor protein.

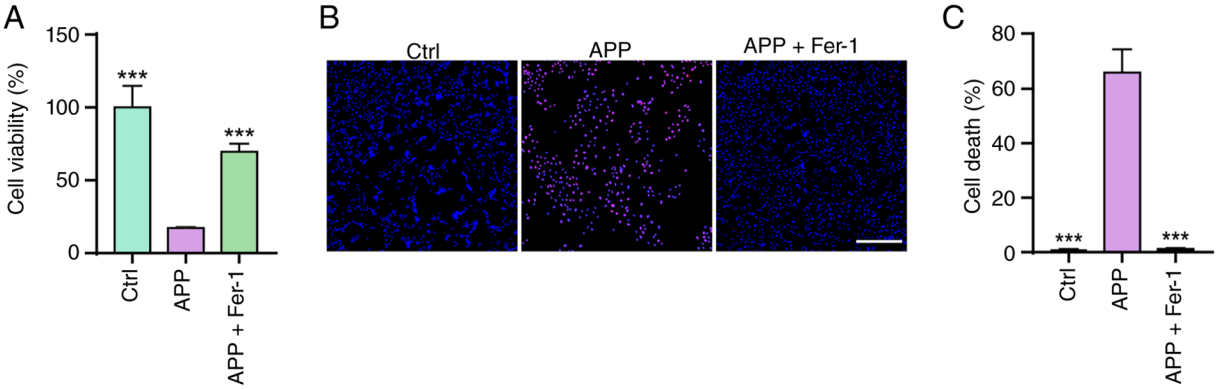

Figure S3. LIP-1 suppresses lipid peroxidation in APP- and A53T-overexpressing SH-SY5Y cells. (A and C) Representative flow cytometry histograms showing lipid peroxidation detected by BODIPY 581/591 C11 staining using the lipid peroxidation assay kit (cat. no. S0043S). FITC-positive cells indicate oxidized BODIPY C11-positive cells with elevated lipid ROS. (B and D) Quantitative analysis of FITC-positive cells in APP- and A53T-overexpressing SH-SY5Y cells, respectively. Data are presented as the mean ± SEM. ***P<0.001. LIP-1, liproxstatin-1; APP, amyloid precursor protein.

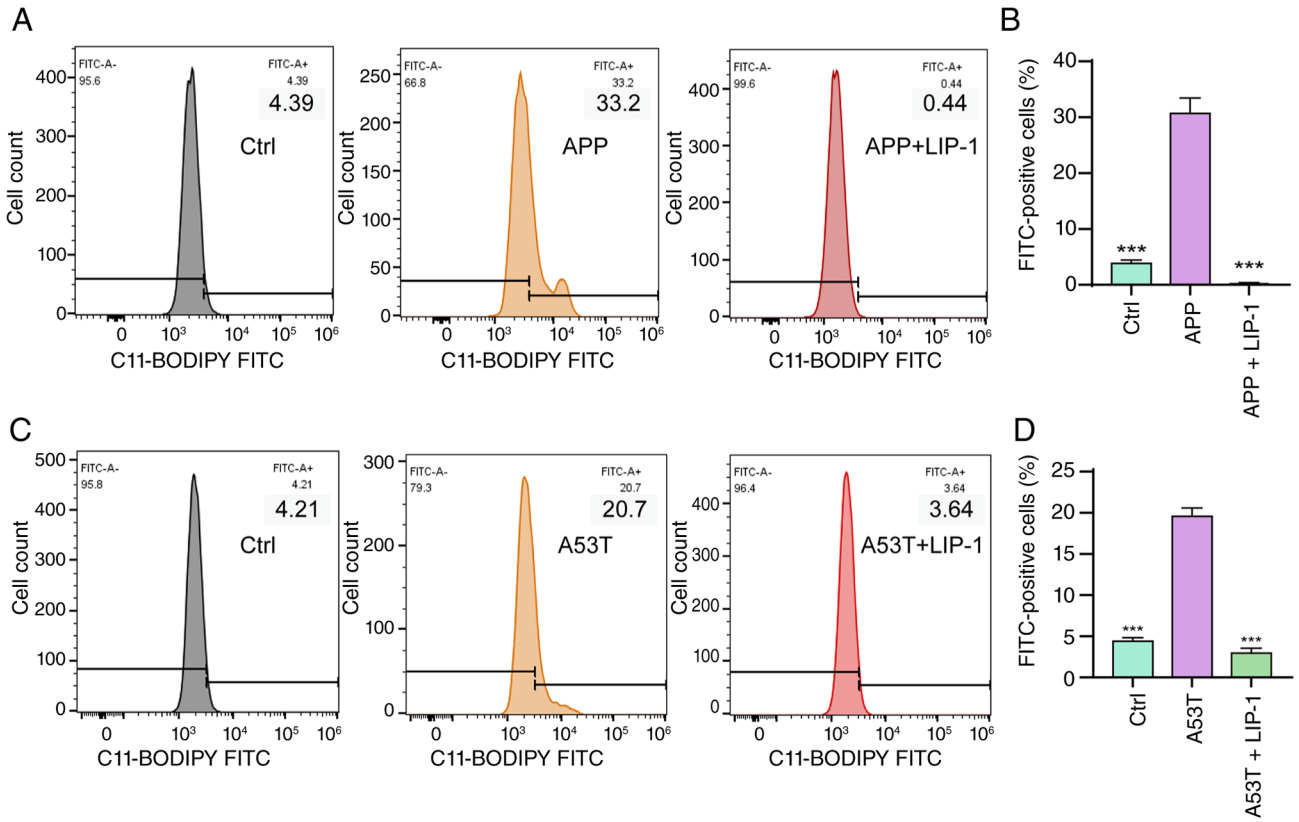

Figure S4. Representative phase-contrast images showing SH-SY5Y cells cultured in medium containing 25 mM or 0 mM glucose with or without erastin (10 μM) treatment for 24 h. Magnification, x10; scale bars, 50 μm.

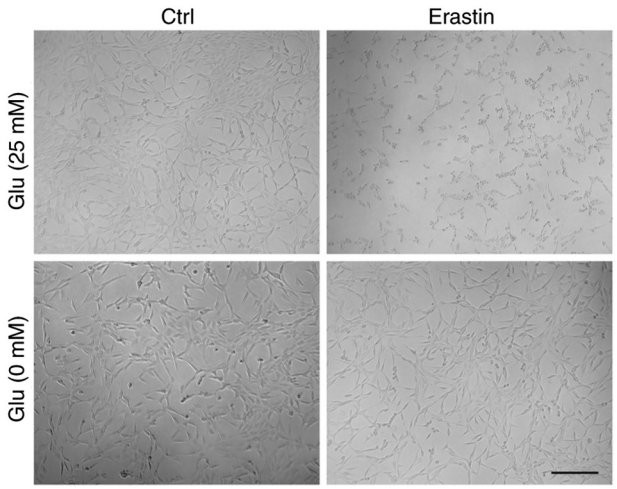

Figure S5. Cell viability of SH-SY5Y cells treated with erastin (A) or RSL3 (B) in the presence of CC or CC + LIP-1. Data are presented as the mean ± SEM. ***P<0.001. CC, Compound C; LIP-1, liproxstatin-1.

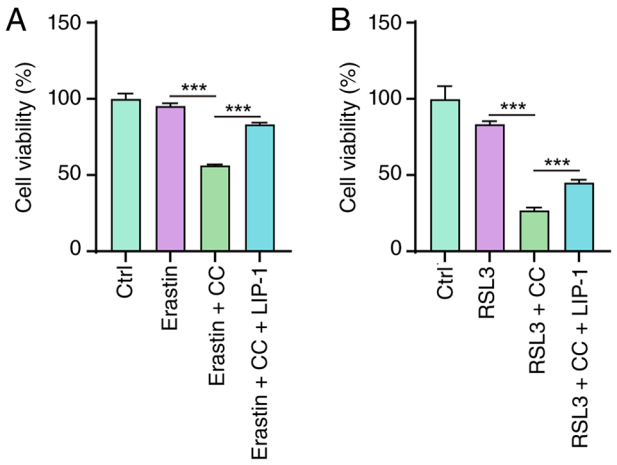

Figure S6. AMPK siRNA efficiently reduces AMPK protein expression in SH-SY5Y cells. (A) Representative western blot analysis of AMPK expression in SH-SY5Y cells transfected with control siRNA (siCtrl) or AMPK siRNA (siAMPK). (B) Quantification of AMPK protein levels normalized to β-actin. Data are presented as the mean ± SEM. $^{**}P<0.01$. AMPK, AMP-activated protein kinase; siRNA, small interfering RNA.

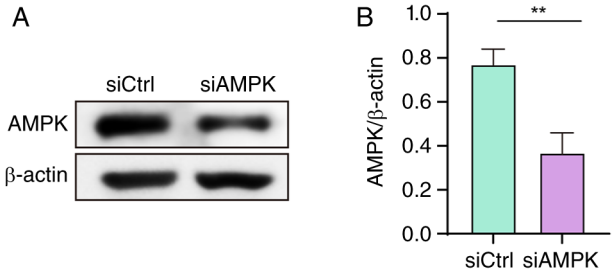

Figure S7. AMPK knockdown weakens the protective effect of glucose deprivation against ferroptotic cell death in SH-SY5Y cells. (A) Representative Hoechst/PI staining images of SH-SY5Y cells transfected with siCtrl or siAMPK and then treated with erastin or RSL3 under normal glucose or glucose-deprived conditions. Magnification, x10; scale bars, 50 μm. (B and C) Quantitative analysis of cell death in erastin-treated and RSL3-treated cells, respectively. Data are presented as the mean ± SEM; ***P<0.001. AMPK, AMP-activated protein kinase; siRNA, small interfering RNA.

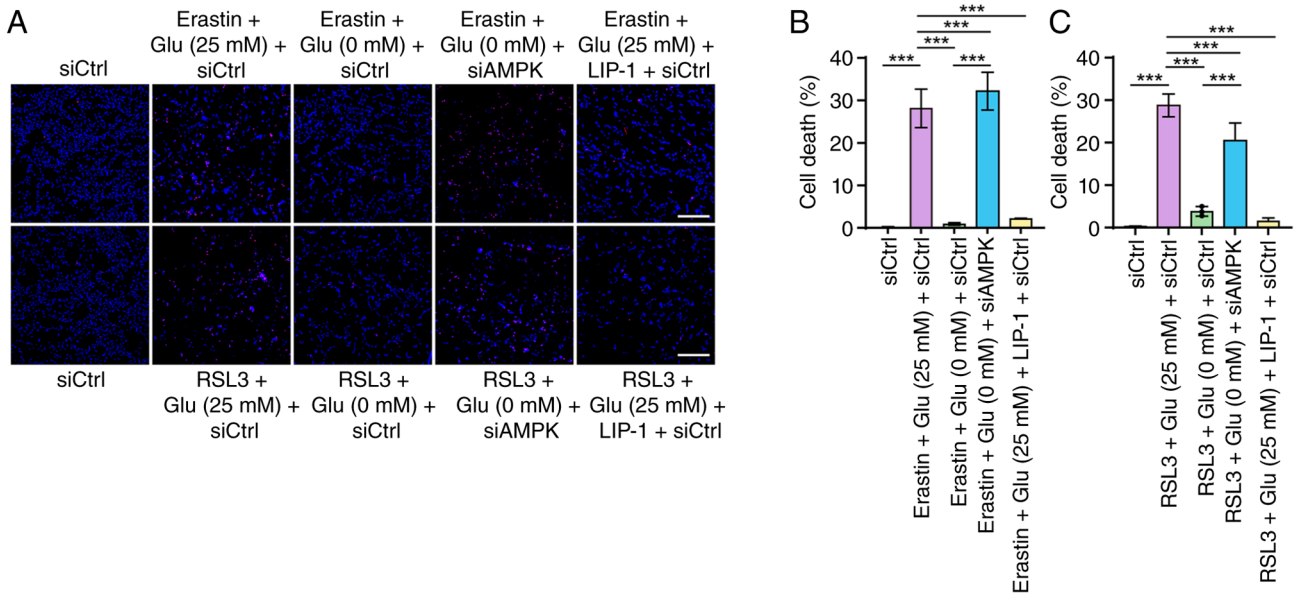

Figure S8. Representative fluorescence images of Hoechst/PI staining (A) and quantification of cell death (B) in erastin-induced SH-SY5Y cells treated with or without AICAR or 2DG. Magnification, x10; scale bars, 50 μm. Data are presented as the mean ± SEM; ***P<0.001. 2DG, 2-deoxy-D-glucose; AICAR, 5-Aminoimidazole-4-carboxamide ribonucleoside.

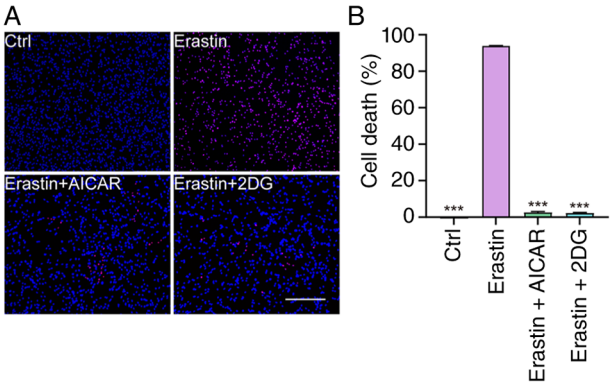

Figure S9. TOFA reduces erastin- or RSL3-induced neutral lipid/lipid droplet accumulation in SH-SY5Y cells. (A) Representative fluorescence images of BODIPY 493/503 staining in SH-SY5Y cells treated with erastin or RSL3 in the presence or absence of TOFA. Magnification, x20; scale bars, 100 μm. (B and C) Quantitative analysis of BODIPY 493/503 fluorescence intensity in erastin-treated and RSL3-treated cells, respectively. Data are presented as the mean ± SEM. ***P<0.001. TOFA, 5-tetradecyloxy-2-furoic acid.

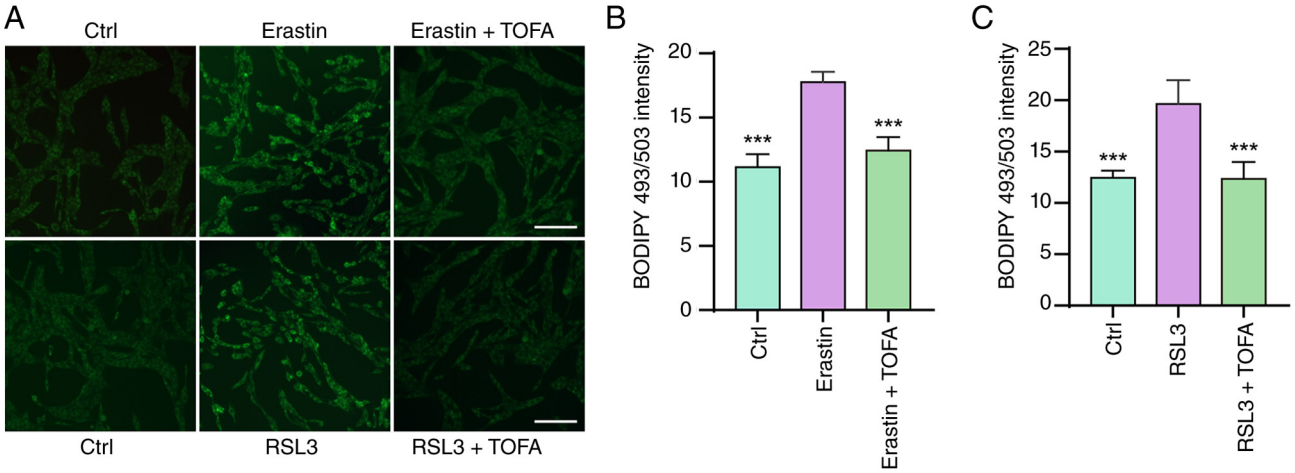

Figure S10. Representative fluorescence images (A) and quantification of fluorescence intensity (B) of SH-SY5Y cells transfected with pEGFP-N1 cultured in medium containing 25 mM or 0 mM glucose for 24 h. Magnification, x10; scale bars, 50 μm. Data are presented as the mean ± SEM. ns, not significant.

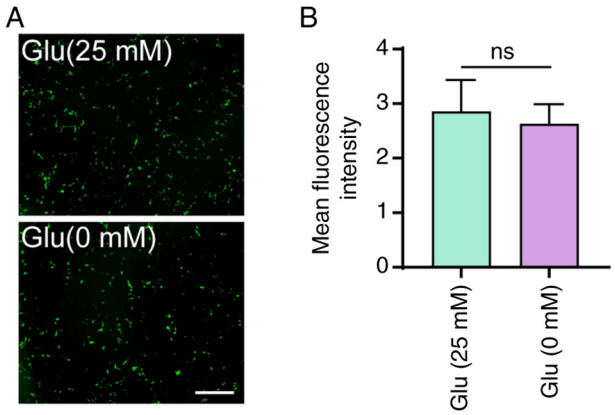

Figure S11. Quantification of MDA content in control, mutant huntingtin Q74-overexpressing, and Q74-overexpressing cells treated with glucose deprivation (0 mM), AICAR, or 2DG. Data are presented as the mean ± SEM. *P<0.05, **P<0.01 and ***P<0.001. 2DG, 2-deoxy-D-glucose; MDA, malondialdehyde; AICAR, 5-Aminoimidazole-4-carboxamide ribonucleoside.

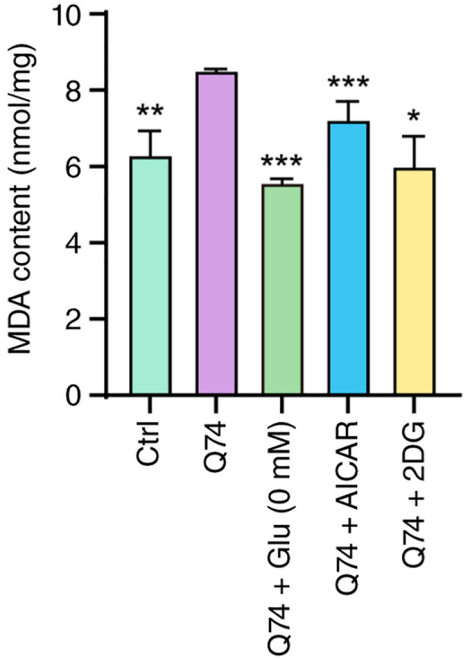

Figure S12. 2DG and LIP-1 reduce MDA levels in proteinopathy *C. elegans* models. (A-C) Quantification of MDA content in *C. elegans* models expressing pathogenic proteins. (A) CL4176 strain expressing human Aβ, (B) NL5901 strain expressing α-synuclein, and (C) AM141 strain expressing polyQ expansion. Worms were treated with or without 2DG (200 μM) or LIP-1 (200 μM). Data are presented as the mean ± SEM. *P<0.05, **P<0.01 and ***P<0.001. 2DG, 2-deoxy-D-glucose; LIP-1, liproxstatin-1; MDA, malondialdehyde.

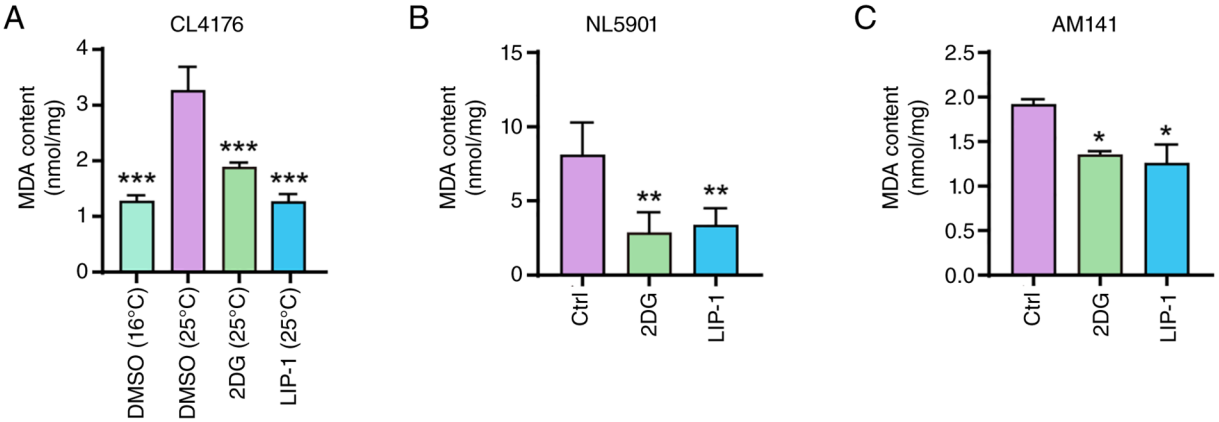

Figure S13. AMPK activation suppresses accumulation of reactive oxygen species and lipid peroxidation in 6-OHDA-induced N2 worms. (A and C) Representative fluorescence images of DHE (A) and C11 BODIPY (C) staining in 6-OHDA-induced N2 worms treated with 2DG (200 μM) or LIP-1 (200 μM). Magnification, x10; scale bars, 50 μm. (B and D) Quantification of DHE fluorescence intensity (B) the green-to-red (G/R) fluorescence ratio of C11-BODIPY 581/591 (D) in N2 worms under the indicated conditions. The G/R ratio represents the oxidized-to-reduced fluorescence ratio and was used as an indicator of lipid peroxidation. Data are presented as the mean ± SEM. ***P<0.001. 6-OHDA, 6-hydroxydopamine; 2DG, 2-deoxy-D-glucose; LIP-1, liproxstatin-1.

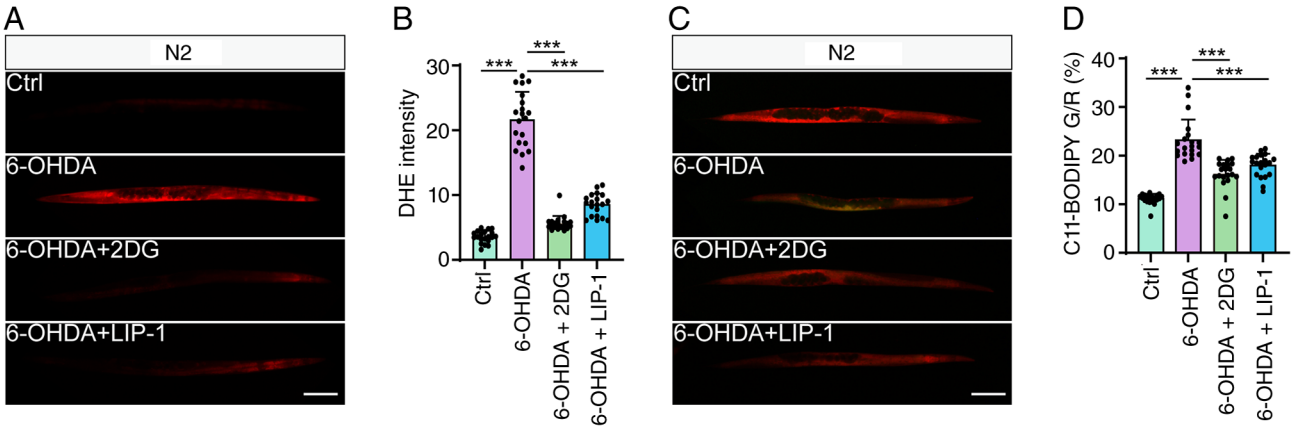

Figure S14. 2DG and LIP-1 preserve dopaminergic neuron viability in 6-OHDA-induced BZ555 worms. (A) Representative fluorescence images of dopaminergic neurons in BZ555 worms following exposure to 6-OHDA with or without 2DG (200 μM) or LIP-1 (200 μM) treatment for 24 h. The GFP signal reflects the integrity of dopaminergic neurons. Magnification, x20; scale bars, 100 μm. (B) Quantification of GFP fluorescence intensity in BZ555 worms. Data are presented as the mean ± SEM from three independent experiments (n=20 worms per group); ***P<0.001. 2DG, 2-deoxy-D-glucose; 6-OHDA, 6-hydroxydopamine; LIP-1, liproxstatin-1.

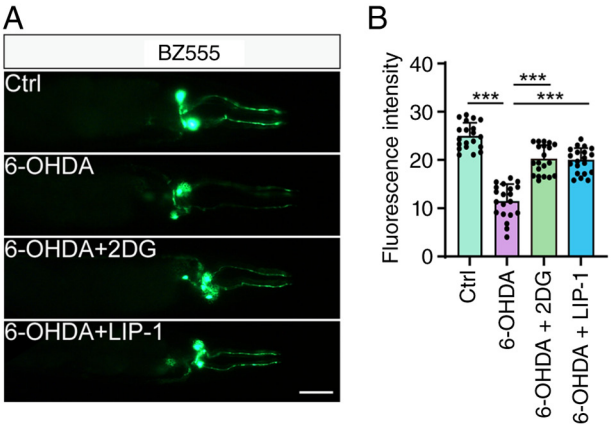

Figure S15. 2DG and LIP-1 alleviate hippocampal CA1 histopathological damage in 3xTg-AD mice. Representative H&E-stained hippocampal sections from WT control, 3xTg-AD, 3xTg-AD + 2DG, and 3xTg-AD + LIP-1 mice. The upper panels show the overall hippocampal architecture, and the dashed boxes indicate the CA1 regions shown at higher magnification in the lower panels. Arrows indicate damaged or pyknotic neurons. Magnification, x5; scale bar, 300 μm. 2DG, 2-deoxy-D-glucose; LIP-1, liproxstatin-1; WT, wild-type; H&E, hematoxylin and eosin.

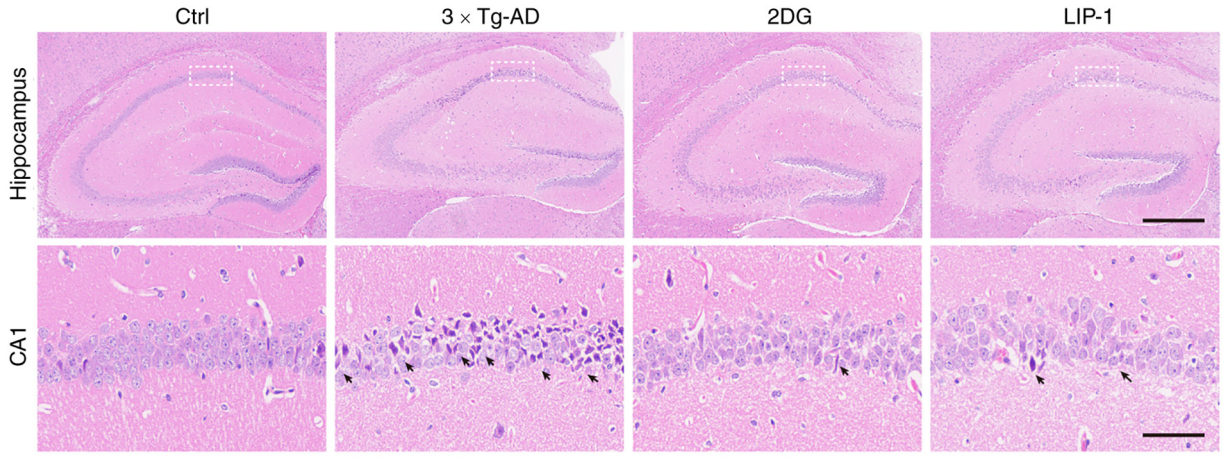

Figure S16. Quantification of the 4-HNE immunohistochemical staining shown in Fig. 7K. Data are presented as the mean ± SEM. ***P<0.001. 4-HNE, 4-hydroxynonenal; 2DG, 2-deoxy-D-glucose; LIP-1, liproxstatin-1.